Nuclear Engineering and Technology 50 (2018) 425–431

Contents lists available at ScienceDirect

Nuclear Engineering and Technology

journal homepage: www.elsevier.com/locate/net

Original Article

Evaluation of axial and tangential ultimate tensile strength of zirconium cladding tubes

Márton Király*, Dániel Mihály Antók, Lászlóné Horváth, Zoltán Hózer

Centre for Energy Research of the Hungarian Academy of Sciences (MTA EK), H-1525 Budapest, P.O. Box 49, Hungary

ARTICLE INFO

Article history:
Received 2 November 2017
Received in revised form
9 January 2018
Accepted 10 January 2018
Available online 31 January 2018

Keywords:
E110
E110G
Finite Element
Tensile Test
UTS
Zirconium Cladding

ABSTRACT

Different methods of axial and tangential testing and various sample geometries were investigated, and new test geometries were designed to determine the ultimate tensile strength of zirconium cladding tubes. The finite element method was used to model the tensile tests, and the results of the simulations were evaluated. Axial and tangential tensile tests were performed on as-received and machined fuel cladding tube samples of both E110 and E110G Russian zirconium alloys at room temperature to compare their ultimate tensile strengths and the different sample preparation methods.

1. Introduction

Anisotropic materials may have significant differences between their tangential and axial ultimate tensile strengths (UTSs), and they should be measured separately. Because zirconium alloy nuclear fuel cladding materials are typically anisotropic due to the production technology, such properties can be determined by longitudinal (axial) and ring (tangential) tensile tests. The most important factors affecting the results of the tensile strength measurement are the temperature of the test, the machining method of the specimens, and—for ring specimens—the friction between the sample and the dies. Another feature is the tensile deformation rate, which can be controlled by the crosshead speed of the universal tensile testing machine. Because the tube geometry is given, the test specimens have to be produced from the tubes. Before tensile tests are carried out, finite element analysis may be required to evaluate the applicability of the tensile test specimen geometry chosen for the tests and improve it if needed.

2. Methodology review

2.1. Axial tensile tests

Several techniques have been developed for axial tensile strength measurement of nuclear fuel cladding tubes. To obtain a well-defined gage section, the tubes are milled to form a reduced section. The samples are pin loaded with pinholes drilled at the sample ends apart from the gage sections. Mostly, tubes with two narrow wings are used, or they can be cut in half into two semi-tubes to be measured separately. During the tensile test, the plastic deformation develops only in the gage sections. The stresses are almost uniform along these sections up to necking. The tensile test data measured this way are often considered to be more accurate. The difficulty of this test lies within the thin cladding from which the test specimens are to be machined. The small size and complex shape of the sample limit the tools and methods usable for the preparation and the achievable accuracy. With the use of fine mechanical Computer Numerical Control (CNC), milling the size of the samples may be considered close to the given nominal value.

It should be noted that axial tensile sample requires usually 10 to 12 times longer tubes than hoop tensile tests. With irradiated material, this can be a problem because the amount of irradiated material available for such tests is limited. It is also known that in general, the irradiation eliminates the anisotropic behavior of the

* *Corresponding author.*
E-mail address: kiraly.marton@energia.mta.hu (M. Király).

https://doi.org/10.1016/j.net.2018.01.002

cladding tubes, and irradiated materials show isotropic behavior after one or two campaigns in the reactor [1]. In this case, the axial tensile test does not seem to be the most economical method of material testing.

It is relatively simple to carry out axial tensile tests because it does not require complex experimental devices, and there is no need to perform complex calculations to interpret the tests. They may also be carried out in normal operation and accident-relevant conditions covering a very wide range of temperatures and strain speeds. However, the determination of the axial stress has significant disadvantages. The material is tested in the longitudinal direction under uniaxial conditions, while in typical simulated accident conditions the cladding failure is mainly due to longitudinal cracks, which suggests that in these cases, the tangential load is dominant.

2.2. Tangential tensile tests

Several techniques have been developed around the world to measure the tangential tensile strength of zirconium cladding tubes. The same characteristics can be defined through the tension test of annular specimens as with the axial samples (yield strength, tensile strength, and total and uniform elongation), but the load is mainly tangential. An important feature of ring tensile testing is that the specimen may deform significantly as the load increases, and it does not keep its original ring geometry.

The tests can be done using full rings or machined test specimens. The benefits of examining narrow rings are that only a small amount of material is needed for each specimen. This is a clear advantage if only limited quantities are available, such as irradiated materials. However, for postirradiation examination of a material's characteristics, especially the measurement of embrittlement, it is clear that the probability that the sample has a weak point (e.g., a hydride blisters) is less in case of a short sample; therefore, more short samples have to be examined to determine the material's behavior instead of a few long samples.

The simplest way to prepare tensile test samples is to cut rings from the tubes; however, machined rings are usually used; therefore, the tensile cross section can be defined more precisely. These are prepared by milling the two sides of the ring, creating two opposite narrow wings. The small size and complex geometry require precision mechanical devices. A number of different procedures have been developed to measure the tensile strengths of such rings.

In the first case (Fig. 1A), the inner diameter of the ring is roughly equal to the circular heads that they are placed on, and the rings are loaded so that the machined section is facing where the two heads meet, perpendicular to the direction of the pull. The disadvantage of this method is that the tensile region of the specimen is deformed and flattened during the test, and the stress is not purely tangential. This approach was used by the French Atomic Energy Agency (CEA) [2] and previously in the AEKI (the predecessor of current MTA EK) [3].

In the second case (Fig. 1B), the same design was used as in the previous one, but the machined parts of the rings are located at the top and bottom of the heads, in the direction of the pull. These tests typically give higher maximum load values than when the machined parts of the rings are to the sides. The friction coefficient between the tensile head and the ring is a critical parameter; therefore, appropriate lubrication must be provided. This type of test is used by the Japan Atomic Energy Agency [4] and the Korea Atomic Energy Research Institute [5].

In the third case, to keep the ring geometry round, an intermediate piece called “dog bone” is used, which prevents the flattening of the narrowed section [6], but it also induces some localized shear depending on the exact geometry (Fig. 1C). With the machined section of the ring specimen placed in the pulling direction perpendicular to the load, the inner diameter of the ring is roughly equal to the curvature of the dog bone piece. However, inserting this dog bone between the dies is difficult, especially considering high temperature measurements. This approach is used by the Argonne National Laboratory (USA) [7] and Studsvik (Sweden) [8].

The fourth kind of test was developed by the National Research Center “Kurchatov Institute” (Russia) [9]. While Western researchers examined mainly Zircaloy alloys, this institute mainly studies Russian cladding alloys (e.g., E110). The distortion of the full, roughly shaped ring in this case is very significant because the mandrel diameter is significantly smaller than the inner diameter of the ring (Fig. 1D). The specimens were not narrowed, but microincisions were used to accurately monitor the deformation of the samples. This approach differs significantly from the others: the maximum bending strength is at the beginning of the test.

3. Materials and methods

Over the past 20 years, numerous mechanical tests have been performed in the AEKI and later in MTA EK on the E110 and the E110G cladding tubes [10]. A significant part of these measurements was performed on oxidized and hydrogenated samples representative of incident and accident conditions.

The zirconium for the currently used E110 cladding alloy is produced 60% through an iodine process and 40% through an electrolytic process. In the iodide method, the gaseous zirconium tetraiodide is condensed on a thin tungsten filament and thermally decomposed, wherein the zirconium metal is deposited on the tungsten (van Arkel–de Boer procedure). During the electrolytic process, potassium hexafluorozirconate ($K_2[ZrF_6]$) or zirconium dioxide is mixed with molten salts (e.g., KCl and NaCl or ZrF4 and NaF), and the zirconium precipitates from the melt on the electrode surface. In the western countries, the Kroll process is widely used, where zirconium tetrachloride is reduced with magnesium, and the residual magnesium in the metal is evaporated in vacuum, leaving a sponge. The zirconium metal in the new E110G cladding comes from this sponge (70%) (in Russian “*Gubka*”, hence the “G”) and the iodide process (30%). The chemical composition of E110G alloy remains the same, 99% zirconium and 1% niobium, but permissible levels of certain trace element concentrations change.

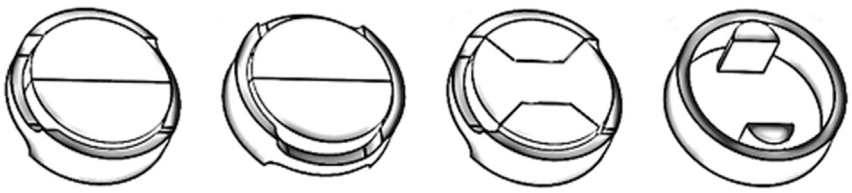

Fig. 1. Four different methods of tangential tensile testing. (A) Side machined ring (B), top-bottom machined ring, (C) side-machined ring with dogbone, (D) small mendrels.

There is no standard method to measure the axial tensile strength of cladding tubes in Hungary; therefore, we decided to develop our own method. The geometry of the samples was determined along the lines of those used in RIAR in Dimitrovgrad [9], but instead of a half tube, we used a 50-mm–long full tube with two 10-mm–long parallel test regions (Fig. 2). To prevent lateral strain in the testing machine, two pins were used to fix the samples.

For the measurement of the tangential tensile strength of the claddings, we decided to replicate the dies used in a similar research program in AEKI (predecessor of MTA EK) [3]. These dies were 3 mm wide; so, only narrow rings could fit on the mandrels.

We used two ring sample geometries, full rings and narrowed rings. The 2-mm–wide full rings were simply cut from the cladding tubes. The geometry of the machined, narrowed rings (Fig. 3) was modeled after the ones used by CEA, but owing to the limitation of the dies, the samples were cut from 2.5-mm–wide rings, with the narrowed section measuring 1 mm wide.

4. Finite element simulation of the tensile tests

4.1. Test specimen geometries

Finite element method (FEM) simulations were carried out on MSC Marc-Mentat 2005 r3 nonlinear finite element analysis software. The main goal was to decide whether or not a given tensile test arrangement is suitable for determining the UTS. Therefore, we evaluated the load–displacement curves and the stress distributions in the pipes and rings during the tensile tests. The UTS was calculated by dividing the maximum load by the as-fabricated cross section of the specimen. Numerous simulations were carried out to analyze the sensitivity of the results, considering the change of geometric parameters and the friction coefficient.

The cladding material in all models was considered homogeneous, and the simulations used nonlinear large strain theory. A linear elastic–plastic strain-hardening material model was chosen. Quantitatively, the anisotropic behavior was not known, but one could assume that the axial and tangential material properties were not highly different;, therefore, as a simplification in the simulations, the cladding material was considered isotropic. The material properties were provided by the manufacturer, but only for the E110 alloy; hence, all the simulations used these values. Young's modulus was given as 96 GPa, and the Poisson ratio was 0.41 at room temperature.

The equation used to generate the flow curve at room temperature was

$$\sigma = K \cdot \varepsilon^{n}$$

where

σ is the equivalent von Mises true stress.
K is the strength coefficient, given as 459 MPa.
ε is the equivalent von Mises true strain.
n is the strain hardening exponent, given as 0.078.

The Considère criterion provides an exact solution for engineering uniaxial tensile strength: UTS $= K \cdot n^{n} \cdot \exp(-n) = 348$ MPa. A hoop or axial tensile test sample machined on tubular geometry is expected to provide a good estimate of this value. Consequently, the adequacy of the sample geometry and loading conditions will be checked by comparing the calculated UTS with a target value equal to 348 MPa.

The models used symmetry planes whenever it was possible to decrease the number of finite element nodes and thus the computation time. Force–displacement (of fastening head) curves and the equivalent von Mises stress fields were collected as results.

4.2. Axial tensile tests

First, the axial tensile test of a full tube was simulated (Fig. 4). An increasing uniform axial displacement was imposed at one end of the tube and a zero imposed axial displacement at the opposite end. The UTS was estimated to be 346.5 MPa which is very close to the Considère criterion's value. However, the problem with the full tube arrangement is the correct gripping of the tube and the uncertainty of the necking's position.

The tensile tests of the machined tubes were also simulated. We examined different contact conditions between the drilled hole's surface and the head that is responsible for passing over the axial

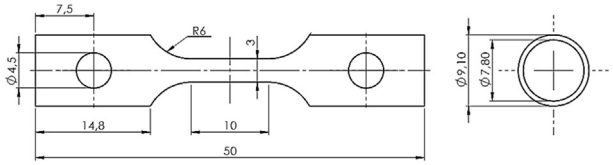

Fig. 2. Drawing of the machined axial test samples.

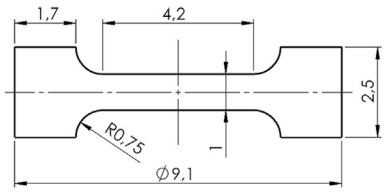

Fig. 3. Drawing of the machined tangential test sample rings.

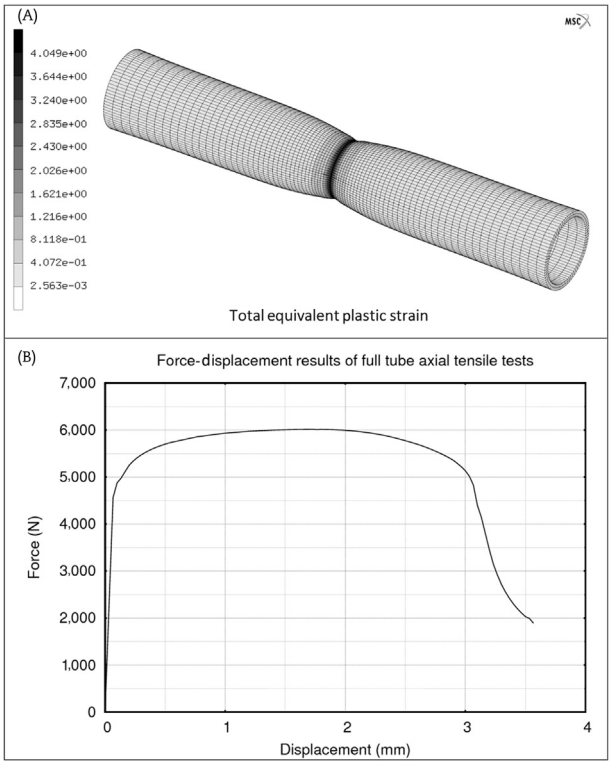

Fig. 4. Modeled axial test of a full tube. (A) The model of the 60-mm–long full tube sample, during the tensile test. (B) The force–displacement curve.

forces (Fig. 5). Several simulations were carried out using different friction coefficients (μ) and different head diameters (D_{head}), while the hole diameter was fixed ($D_{hole} = 2.5$ mm). $\Delta D = D_{hole} - D_{head}$. In cases where it was not mentioned, the default values for these parameters were $\mu = 0.3$ and $\Delta D = 0.2$ mm.

The stress field in the vicinity of the hole is slightly dependent on D_{head}. However, significant deformation near the holes is not expected due to the correctly chosen width of the gauge length. The force–displacement curves indicate that the maximum force value is not sensitive to the head diameter. The axial tensile tests are insensitive to the friction coefficient (the curves are identical, thus not depicted) because the contact surfaces do not slide on each other during the test.

The UTS was 347.6 MPa which was in good agreement with the Considère criterion.

4.3. Ring tensile tests

Three cases of ring tensile tests were simulated: full rings, rings with the machined narrowed regions on the side of the dies (Fig. 6), and machined rings with the narrowed regions on top of the dies. We analyzed the role of the friction coefficient and the diameter difference between the ring and the mandrel.

None of the three cases were sensitive to the difference between the inner diameter of the ring and the diameter of the head (ΔD), and the force–displacement curves (not shown here) indicated that the maximum force was the same for each scenario. The inner diameter of the used die was 7.5 mm; therefore, the difference between the diameter of the die and the inner diameter of the rings (ΔD) in the actual case was between 0.10–0.15 mm.

As with the axial simulations, neither the full nor the side-machined rings were affected by the change of friction coefficient (μ) as the contact surfaces did not slide on each other during the test.

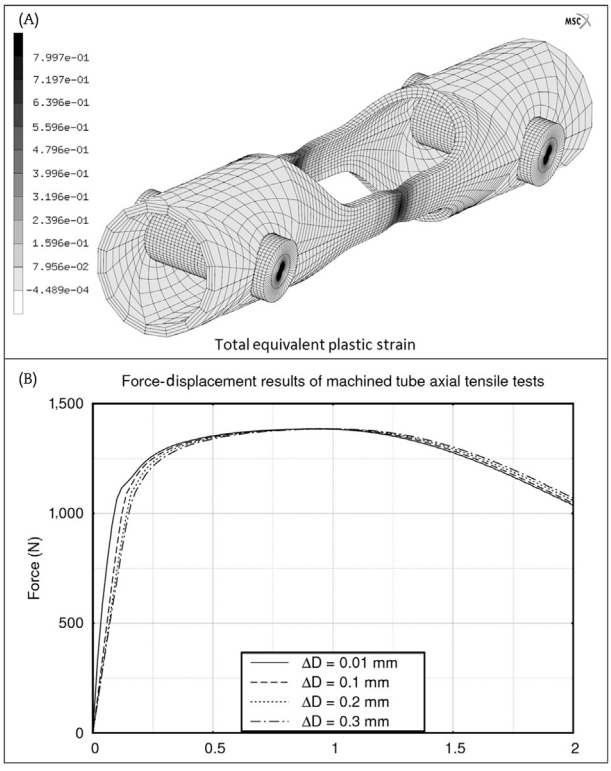

Fig. 5. Model of the axial sample. (A) The model of the 50-mm machined axial tensile testing cladding sample during the tensile test. (B) The force–head-displacement curves in relation with the diameter of the fastening head.

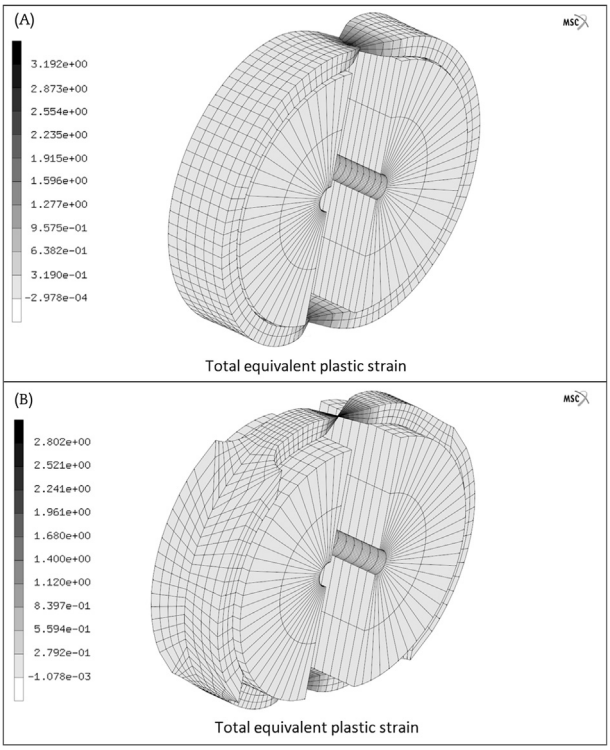

Fig. 6. Models of the ring samples. (A) The models of the 2-mm full ring with the narrowed sections to the sides during the tensile test. (B) The models of the 2-mm machined ring with the narrowed sections to the sides during the tensile test.

The calculated UTSs for the full and the side-machined rings were 344.6 MPa and 343.1 MPa, respectively.

In the case of the machined rings with the narrowed sections resting on the dies (top-bottom method), the contact surfaces slid on each other during the test; therefore, the results are highly dependent on the friction coefficient (Fig. 7). Furthermore, the UTS could not be calculated because the machined cross section of the ring was not perpendicular to the load.

In the experiments done by the Japan Atomic Energy Agency [4] and the Korea Atomic Energy Research Institute [5], they used different methods, such as Teflon tape and graphite vacuum grease to reduce the friction coefficient, but these methods are not applicable for high temperature measurements above 240°C. In MTA EK, we planned to do tensile testing at room temperature and later at higher temperatures up to 300°C (near the operating temperature of 300–330°C); so, this method could not be used.

It is clear that the maximal forces estimated using different geometries were in good agreement with the values estimated by the Considère criterion (within ~1% difference). The FEM models suggested that the UTSs of the tubes and rings could be evaluated with the designed tensile test geometries.

5. Experimental setup

To compare the mechanical properties of the untreated E110 and E110G cladding alloy tube samples, tensile strength tests were carried out to determine their UTS in the axial and tangential directions at an ambient temperature.

The axial specimens from the E110 and the E110G alloy tubes were at first prepared by manual milling and later by CNC milling.

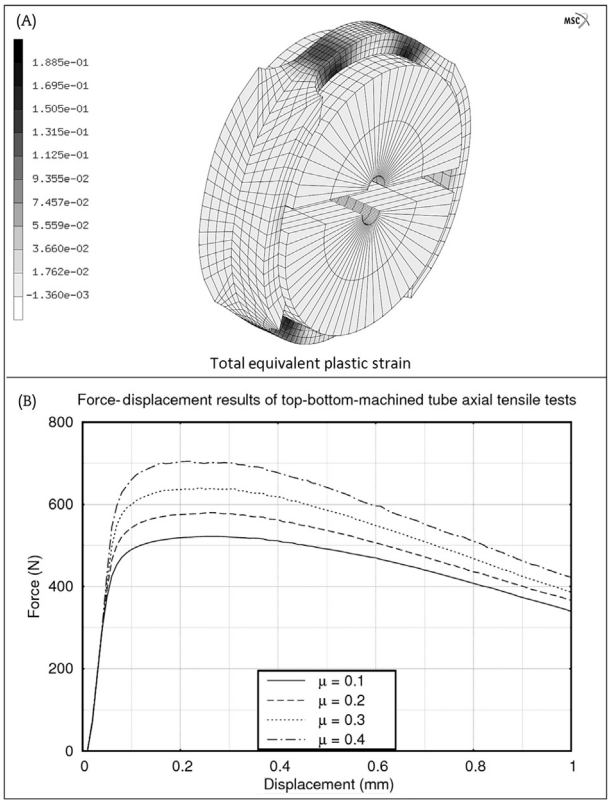

Fig. 7. The top-bottom machined ring sample. (A) The model of the top-bottom machined rings with the narrowed section on the dies during the tensile test. (B) The force–displacement curves in relation with the friction coefficient.

Owing to the slow machining, the samples underwent minimal heat treatment during fabrication.

The full rings were cut from the cladding tubes by lathe and then polished to give a smooth cut surface. The machined ring samples were prepared by CNC milling, and some E110G alloy rings were prepared by electro discharge machining (EDM). Unfortunately, during the EDM, the rings suffered significant thermal treatment (over 900°C) and slight oxidation as they began to glow during preparation. The phase transition of zirconium starts above 780°C, and therefore, this heat treatment could have a significant effect on the UTS. The thickness of the oxide layer that covered their surfaces is unknown, and the color of the oxide was mostly black with some light blue areas on the inside of the rings.

All the tensile tests were carried out using an Instron 1195 universal testing machine, and the pulling rate was 0.5 mm/min (Fig. 8). The E110 and E110G samples were tested at room temperature to compare the tensile strength values resulting from the different sample geometries.

6. Results

6.1. Axial tensile tests

The results of the axial tensile tests are summarized in Table 1 and Fig. 9. Axial tensile strength values obtained from the full pipe and the machined samples were in good agreement for the two alloys with a 1% relative standard deviation. The two symmetrical wings of the tensile test specimens stretched and tore almost identically at the same load, which supports the results of the modeling.

We calculated 430.1 MPa axial UTS for the E110G alloy and 385.9 MPa for the E110 alloy at room temperature from the full tube and the milled axial samples. The UTS calculated from the CNC milled axial samples was 6% higher for both alloys. For both tests

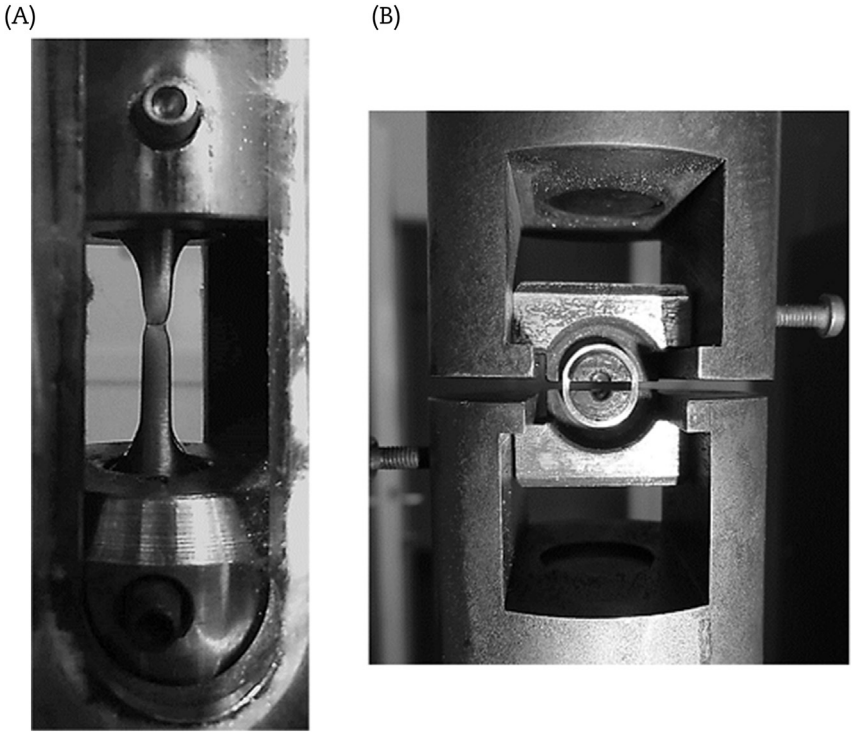

Fig. 8. Testing equiplent and samples during tensile test. (A) The 50-mm–long machined axial cladding samples during tensile test. (B) The 2-mm–wide full ring cladding samples during tensile test.

Table 1
The results of the axial tensile tests.

Material	Sample type	UTS (MPa)
E110	Full tube	385.3
	Milled axial	381.2
		391.2
	CNC axial	405.5
		410.8
E110G	Full tube	427.6
	Milled axial	429.5
		433.2
	CNC axial	454.9
		459.2

CNC, Computer Numerical Control; UTS, ultimate tensile strength.

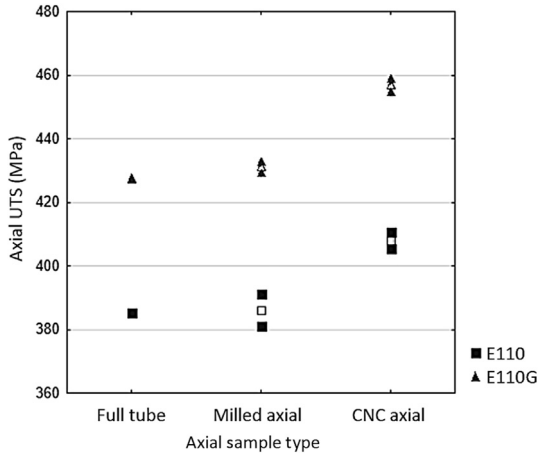

Fig. 9. The results of the axial tensile tests.
CNC, Computer Numerical Control; UTS, ultimate tensile strength.

the axial UTS of the E110G alloy samples was on average 11% higher than that for the E110 samples.

6.2. Ring tensile tests

The results of the tangential tensile tests are summarized in Table 2 and Fig. 10. The two symmetrical wings of the full and machined rings stretched and tore almost identically at the same load, which also supports the results of the finite element modeling. Only the side-mounted rings method was used as the top-bottom method (described previously) was found to be not usable for the determination of the UTS.

Table 2
The results of the tangential tensile tests.

Material	Sample type	UTS (MPa)
E110	Full ring	358.6
		358.9
		364.5
	CNC ring	341.9
		347.3
		328.2
		325.6
		340.2
E110G	Full ring	409.1
		402.2
		405.2
	CNC ring	400.1
		414.3
		393.7
		393.8
		397.4
	EDM ring	429.0

CNC, Computer Numerical Control; EDM, electro discharge machining; UTS, ultimate tensile strength.

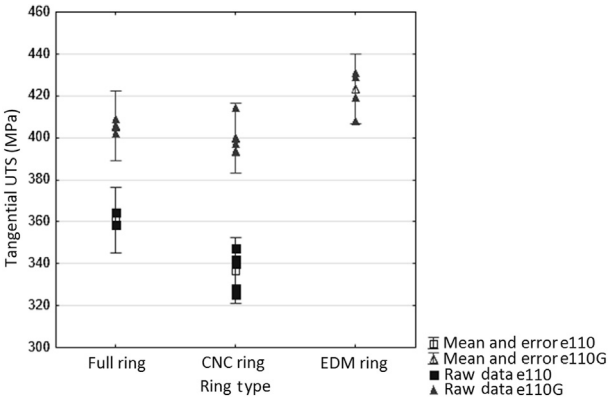

Fig. 10. The results of the tangential tensile tests.
CNC, Computer Numerical Control; EDM, electro discharge machining; UTS, ultimate tensile strength.

The tangential UTS calculated from the testing of full rings was 405.5 MPa for the E110G alloy and 360.6 MPa for the E110 alloy at room temperature. The tangential UTS of the E110G alloy samples was on average 11% higher than that for the E110 samples, a result similar to the axial tests.

For the machined rings, the average measured tangential UTS of the CNC-machined rings was 336.6 MPa for E110 and 399.8 MPa for E110G. The deviation from the measurements using full rings is negligible for E110G, but the measured tensile strength for E110 using full rings was 6% higher than that was before. The average measured tangential UTS of the EDM-machined E110G alloy rings was 423.4 MPa. This higher tensile strength could be attributed to the heat treatment and surface oxidation that occurred during sample fabrication.

7. Discussion

The three main goals of this research were achieved: the mechanical properties of the two Russian cladding alloys were evaluated and compared, the anisotropy of the cladding materials was demonstrated, and new tensile test sample geometries were evaluated and tested.

The standard deviation of the tensile tests was quite high, even though three parallel measurements were made, and therefore, the UTS can only be calculated with a 5% relative error.

The difference between the various sample geometries could be attributed to the method of sample preparation and the heat treatment and surface oxidation of the samples during cutting and machining. Special care has to be taken during these steps as the difference between the heating up of the samples could lead to significant error.

For both alloys, the tensile strength measured in the hoop direction was about 6% lower than that measured axially. This is due to the anisotropy of the cladding tubes.

Our calculated 385.9 MPa average UTS for the axial E110 samples was in good agreement with the data available in various other databases. These measurements were conducted using either cladding tubes or flattened standardized tensile samples measured in the axial direction. The values found in the literature are collected in Table 3.

Table 3
The UTS values found in the literature for the E110 alloy at room temperature.

Publication (date)	UTS (MPa) at 297 K
Thorpe and Smith (1978) [11]	393
Nikulina et al. (1996) [12]	380
Vesely et al. (1998) [13]	407
Kaplar et al. (2001) [1]	378
AEKI (1999) [3]	371
MTA EK (current)	***386***

8. Conclusion

Different methods of axial and tangential testing and sample geometries were investigated using the FEM, and the results of the simulations were evaluated. New axial and tangential test geometries were designed to determine the UTS of zirconium cladding tubes.

Based on the results of the models, machined fuel cladding tube samples were prepared using different methods, and axial and tangential tensile tests were carried out on both E110 and E110G Russian zirconium alloy tubes at room temperature. The UTSs of both alloys were determined using different sample geometries.

The two tested cladding alloys differed substantially. Both the axial and the tangential UTS calculated for the E110G alloy samples were on average 11% higher than that for the E110 samples. For both alloys, the UTS in the hoop direction was 6% lower than the axial UTS. This was attributed to the anisotropy of the cladding material.

The different axial and tangential sample geometries were tested successfully and could be adopted for further experiments. However, great care should be given to the sample preparation to avoid the heating up of the samples during cutting and machining.

Conflict of interest

There is no conflict of interest.

Acknowledgments

The work was supported by the Paks Nuclear Power Plant.

Appendix A. Supplementary data

Supplementary data related to this article can be found at https://doi.org/10.1016/j.net.2018.01.002.

References

[1] A. Kaplar, L. Yegorova, K. Lioutov, A. Konobeyev, N. Jouravkova, Mechanical Properties of Unirradiated and Irradiated Zr-1% Nb Cladding, NUREG/IA-0199, 2001.
[2] J. Desquines, B. Cazalis, C. Bernaudat, C. Poussard, X. Averty, P. Yvon, Mechanical properties pf Zircaloy-4 PWR fuel cladding with burnup 54–64 MWd/kgu and implications for RIA behavior, in: Zirconium in the Nuclear Industry, 14th International Symposium, 2004.
[3] A. Griger, L. Maróti, L. Matus, P. Windberg, Ambient and high temperature mechanical properties of ZrNb1 cladding with different oxygen and hydrogen content, Enlarged Halden Programme Group Meeting 24th -29th May 1999, Loen.
[4] E. Hamanishi, True stress vs true strain analysis with results of ring tensile tests, in: Fuel Safety Research Meeting, April 2006. Tokai (Japan).
[5] Sun-Ki Kim, Je-Geon Bang, Dae-Ho Kim, Yong-Sik Yang, Kun-Woo Song, Do-Sik Kim, Mechanical property evaluation of high burn-up nuclear fuel cladding using the ring tensile test, Met. Mater. Int. 15 (4) (August 2009) 547–553.
[6] Bong-Kook Bae, Sung-Keun Cho, Chang-Sung Seok, A study on ring tensile specimens, Mater. Sci. Eng. A 483–484 (2008) 248–250.
[7] S. Majumdar, R. Daum, M. Billone, Update of ANL approach to derivation of stress-strain curves from ring-stretch tensile tests, in: 6th Mechanical Properties Expert Meeting, October 2005. Kyoto (Japan).
[8] V. Grigoriev, R. Jakobsson, B. Josefsson, D. Schrire, Advanced techniques for mechanical testing of irradiated cladding materials, in: Advanced Post-irradiation Examination Techniques for Water Reactor Fuel, Proceedings of an IAEA Technical Committee Meeting, Dimitrovgrad, May 2001, pp. 14–18.
[9] L. Yegorova, et al., Database on the Behavior of High Burnup Fuel Rods With Zr1%Nb Cladding and UO2 Fuel (VVER Type) Under Reactivity Accident Conditions, NUREG/IA-0156, Vol. 2, July 1999.
[10] Zoltán Hózer, E. Perez-Feró, Cs Győri, L. Matus, L. Vasáros, P. Windberg, L. Maróti, M. Horváth, I. Nagy, A. Pintér-Csordás, T. Novotny, Experimental Database of E110 Claddings Under Accident Conditions AEKI-FRL-2007-123-01/01, NEA-1799/01 IFPE/AEKI-EDB-E110. Documentation, Hungarian Academy of Sciences KFKI Atomic Energy Research Institute, Budapest, 2007.
[11] R. Thorpe, I.O. Smith, Tensile properties of Zr-wt1%Nb alloy, J. of Nuclear Materials 78 (1978) 49–57.
[12] A.V. Nikulina, V.A. Markelov, M.M. Peregud, Y.K. Bibiasvili, V.A. Kotrehkov, A.F. Lositsky, N.V. Kuzmenko, Y.P. Shevin, V.K. Shamardin, G.P. Kobylyansky, A.E. Novoselov, Zirconium alloy E635 as a material for fuel rod cladding and other components of VVER and RBMK Cores Zirconium in the nuclear industry: eleventh International Symposium, in: E. Ross Bradley, G.P. Sabol (Eds.), ASTM STP1295, 1996, pp. 785–804.
[13] J. Vesely, M. Valach, Z. Frejtich, V. Priman, Creep Properties of Non-Irradiated ZrNb1 Cladding Tubes under Normal and Abnormal Storage Conditions, vol. 1089, International Atomic Energy Agency -Publications- IAEA TECDOC, 1998, pp. 305–312.